Electronic Supplementary Material (ESI) for Soft Matter.

Gecko adhesion: a molecular-simulation perspective on the effect of humidity

Tobias Materzok,*,† Stanislav Gorb,*,‡ and Florian Müller-Plathe*,†

†*Eduard-Zintl-Institut für Anorganische und Physikalische Chemie and Profile Area Thermofluids and Interfaces, Technische Universität Darmstadt, Alarich-Weiss-Str. 8, D-64287 Darmstadt, Germany*

‡*Zoological Institute Functional Morphology and Biomechanics, Kiel University, Am Botanischen Garten 1-9, D-24118 Kiel, Germany*

E-mail: t.materzok@theo.chemie.tu-darmstadt.de; sgorb@zoologie.uni-kiel.de; f.mueller-plathe@theo.chemie.tu-darmstadt.de

1 Gecko Keratin Model Creation Procedure

Since one CR bead represents one dimer, each CR bead is covalently bonded to two head regions and two tail regions. The first AM bead in the squence of either the head or tail region is placed orthogonal to the direction of the nanofibrils with a 90 degrees angle between each sequence. The initially placed AM beads are extended by a self-avoiding random walker until all AM beads are fitted into the simulation box. The resulting structure may contain hotspots which are relaxed in the equilibration protocol for the dry gecko keratin (Section S3).

2 Insertion of Water into Gecko Keratin

We step-wise insert water beads such that the resulting interaction with the whole system is favorable $\Delta E_{\text{insertion}} \leq 0$. Thus we only insert beads beyond the Lennard-Jones radius σ of both, the keratin model (CR and AM) and the water beads inserted in previous steps. We use a slightly modified Boltzmann-inverted Lennard-Jones potential (Equation S1) of the Water-Amorphous (W-AM) interaction as a probability density function to efficiently find low energy positions inside the keratin close to AM beads. Then we check if these insertion points would result in favorable interactions $\Delta E_{\text{insertion}}$.

$$P(x) = 1 - \exp\left[12\left(\left(\frac{\sigma_{\text{W-AM}}}{x}\right)^{12} - \left(\frac{\sigma_{\text{W-AM}}}{x}\right)^{6}\right)\right] \tag{1}$$

The amount of water beads inserted at each step, depends on the free volume inside the keratin. After each insertion step we subsequently perform NPT equilibration runs for 0.25 ns each (computational details are described below). Then we repeat the insertion of water beads in this NPT equilibrated wet keratin model. We repeat these two steps (insertion of water beads and subsequent NPT equilibration) until the desired water content is reached.

3 Dry Gecko Keratin Equilibration

In the first step, the AM beads of the initial dry gecko keratin configuration (three-dimensional orthorhombic boundary conditions) are energy minimized using steepest descent until the maximum force is below 100 $\mathrm{kJ\,mol^{-1}\,nm^{-1}}$. The resulting structure is quickly relaxed at 0 K in the microcanoncial ensemble with a small time step of 1 fs for 1 ns while keeping the CR beads fixed.

After scaling the Lennard-Jones interaction parameters (Section 2.3) the equilibration protocol of Endoh et al.[1] is used, with a longer equilibration, by using smaller time steps in the beginning (5 fs instead of 15 fs) and increasing the last NPT equilibration from 7.5 ns to 100 ns. A Berendsen thermostat[2] with a time constant for coupling the temperature of $\tau_T = 1$ ps and a simulation time step of 5 fs is employed to simulate the system at 2000 K for 150 ns in the NVT ensemble. This is done to relax unphysical frustrations[1]. Following the NVT relaxation, the system is cooled down to 300 K in steps of 50 K with a time step of 10 fs. Each cooling step is performed over 3 ns and the final step at 300 K is run for 7.5 ns. Next, a semi-isotropic Berendsen barostat[2] with a coupling time of $\tau_p = 5$ ps and a compressibility of $4.5 \cdot 10^{-5}$ $\mathrm{bar^{-1}}$ is used to equilibrate the system in NPT over 100 ns at 1 bar. The density converges after 30 to 40 ns to 1274 $\mathrm{kg\,m^{-3}}$, similarly, Lennard-Jones interactions converge also after 30 to 40 ns.

4 Wet Gecko Keratin Equilibration

To swell the dry keratin model with water, we insert water beads into the NPT equilibrated dry keratin system, under 3D PBC. With our target of 10% water content we need to add 4123 water beads, in total, into the model. However, in the first step we only insert on average 351 water beads into the dry keratin system (in the fifth step we insert on average 246 beads and in the twentieth step just 143 beads in the wet keratin), because we only insert water beads such that the systems energy is favorable upon insertion. After each insertion

step we run a NPT equilibration for 0.25 ns. By adding just a small number of water beads, at one time, into a system of 22528 keratin beads, under the restrictions described above, the pressure, volume, density and all energetic terms converge in just under 100 ps. The short NPT equilibrations are performed with a time step of 5 fs. A Berendsen thermostat and a semi-isotropic Berendsen barostat[2] are used to keep the system at 300 K and 1 bar. A time constant for coupling the temperature of $\tau_T = 1$ ps and coupling time of the barostat of $\tau_p = 1$ ps with a compressibility of $4.5 \cdot 10^{-5}$ bar^{-1} is adopted. After the last insertion step, we extend the NPT equilibration of the wet keratin by simulating the system for an additional 50 ns with a time step of 10 fs.

Table S1: Range of pulling velocities used in the force probe molecular dynamics simulations and the corresponding loading rates, given the spring constant $k_{\text{pull}} = 5000$ kJ mol^{-1} nm^{-2}. The pulling velocity is the velocity with which the virtual particle is moved away from the surface. This virtual particle is linked with a harmonic spring to the center of mass of the top layer of the nanofibrils.

Pulling velocity v (µm s^{-1})	Loading rate $\dot{F}$ (pN s^{-1})
$3 \cdot 10^5$	$2.5 \cdot 10^{12}$
$5 \cdot 10^5$	$4.5 \cdot 10^{12}$
$7 \cdot 10^5$	$5.8 \cdot 10^{12}$
$1 \cdot 10^6$	$8.3 \cdot 10^{12}$
$3 \cdot 10^6$	$2.5 \cdot 10^{13}$
$5 \cdot 10^6$	$4.2 \cdot 10^{13}$
$7 \cdot 10^6$	$5.8 \cdot 10^{13}$
$1 \cdot 10^7$	$8.3 \cdot 10^{13}$
$3 \cdot 10^7$	$2.5 \cdot 10^{14}$

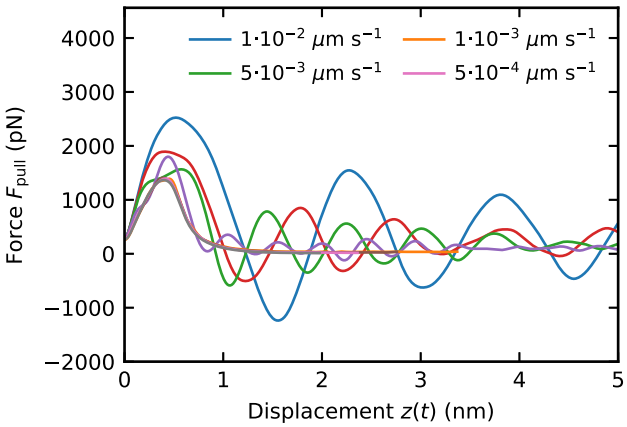

Figure S1: Smoothed force profiles as a function of virtual particle displacement $z(t)$ at different pulling velocities. The maximum at the beginning of each curve corresponds to the unbinding event of the gecko keratin from the hydrophobic octadecyltrichlorosilane self-assembled monolayer. The fast pulling velocities show periodic oscillations after the maximum force, due to keratin oscillating in the harmonic potential around the linked virtual particle. The slowest pulling velocities converge almost immediately to zero after the maximum, by quickly dissipating the forces internally. All forces eventually decay to zero after detachment.

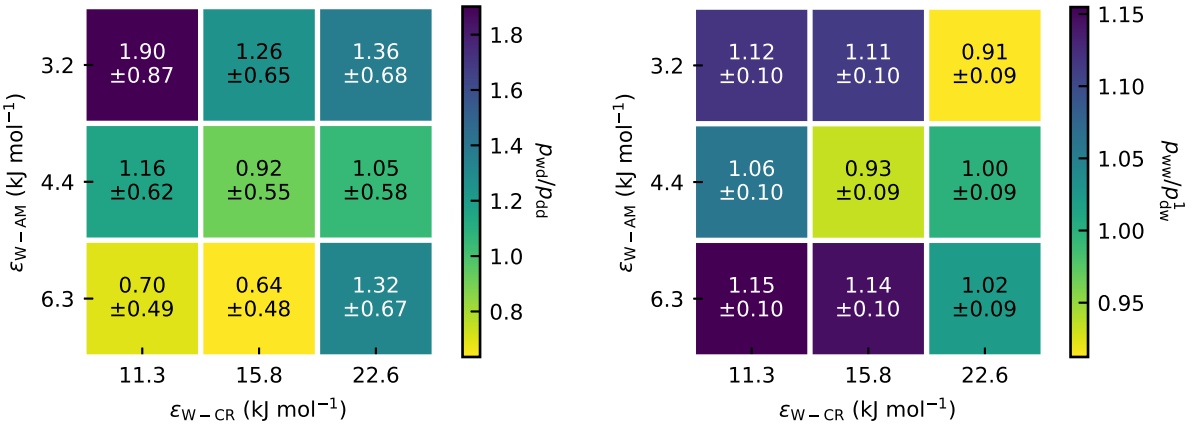

Figure S2: (A) Pull-off pressures of wet keratin attached to a dry surface p_{wd} relative to the pull-off pressure of dry keratin on a dry surface p_{dd} at different Lennard-Jones interaction energies ϵ for Water-Core (W-CR) and Amorph-Water (W-AM) interactions. (B) Pull-off pressures of wet keratin on a wet surface p_{ww} relative to the pull-off force of dry weakly hydrophilic keratin on a wet surface p_{dw}^{1} shows the influence of wet keratin on the pull-off force in the context of a wet surface. Wet gecko keratin on both a dry and a wet surface leads to increased pull-off pressures compared to dry gecko keratin.

Table S2: Results of the force probe molecular dynamics simulations of the wet and dry models. Nomenclature for the type works as follows, the first index classifies if the keratin itself is dry (d) or wet (w), the second index classifies the surface as dry (d) or wet (w). Lennard-Jones interaction parameters of the dry gecko keratin model AM-AM interaction and the interactions of MARTINI water with the gecko keratin model. The Lennard-Jones interaction energies ϵ are in units kJ mol^{-}1. The pull-off force F (in pN) computed for a loading rate of $2.5 \cdot 10^{12}$ pN s^{-1} predicted by Bell+friction fits. Each Bell+friction model was fitted to the most probable pull-off forces of loading rates spanning three orders of magnitude. The standard deviation $\bar{\sigma}$ is computed from five different equilibrations. By using the surface area of the simulation box A, the pull-off forces can be compared between systems as pull-off pressures $p = F/A$, which shows that the change in surface area due to the swelling of the keratin is not large enough to change any trends if one only compares pull-off forces, instead of pull-off pressures.

Type	$\epsilon_{\mathrm{AM-AM}}$	$\epsilon_{\mathrm{W-CR}}$	$\epsilon_{\mathrm{W-AM}}$	F (10^3 pN)	$\bar{\sigma}$ (pN)	A (nm^3)	p (pN nm^{-3})
dd	7.2	-	-	6	456	290.4	2.2
dd	8	-	-	9	456	289.7	3.2
dd	8.8	-	-	9	456	289.2	3.0
dd	9.6	-	-	6	456	288.7	2.2
dd	10.4	-	-	5	456	288.1	1.7
wd	8	11.3	6.3	16	456	298.7	5.3
wd	8	11.3	3.2	22	456	297.1	7.3
wd	8	11.3	4.4	15	456	299.1	4.9
wd	8	15.8	6.3	12	456	298.2	4.0
wd	8	15.8	3.2	13	456	298.8	4.5
wd	8	15.8	4.4	11	456	296.6	3.5
wd	8	22.6	6.3	15	456	301.0	5.1
wd	8	22.6	3.2	8	456	294.0	2.7
wd	8	22.6	4.4	7	456	295.9	2.5
ww	8	11.3	6.3	74	520	298.7	24.6
ww	8	11.3	3.2	90	520	297.1	30.2
ww	8	11.3	4.4	90	520	299.1	30.0
ww	8	15.8	6.3	80	520	298.2	27.0
ww	8	15.8	3.2	85	520	298.8	28.6
ww	8	15.8	4.4	75	520	296.6	25.2
ww	8	22.6	6.3	83	520	301.0	27.6
ww	8	22.6	3.2	92	520	294.0	31.2
ww	8	22.6	4.4	91	520	295.9	30.9
dw	8	11.3	3.2	78	520	289.8	27.0

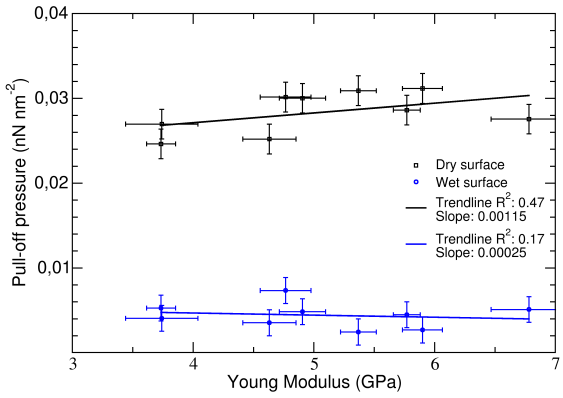

Figure S3: Pull-off pressures of wet gecko keratin as a function of Young modulus from the dry (black) and wet (blue) hydrophobic surface. Difference in the elastic modulus are due to different hydrophilicities of our wet gecko keratin model.

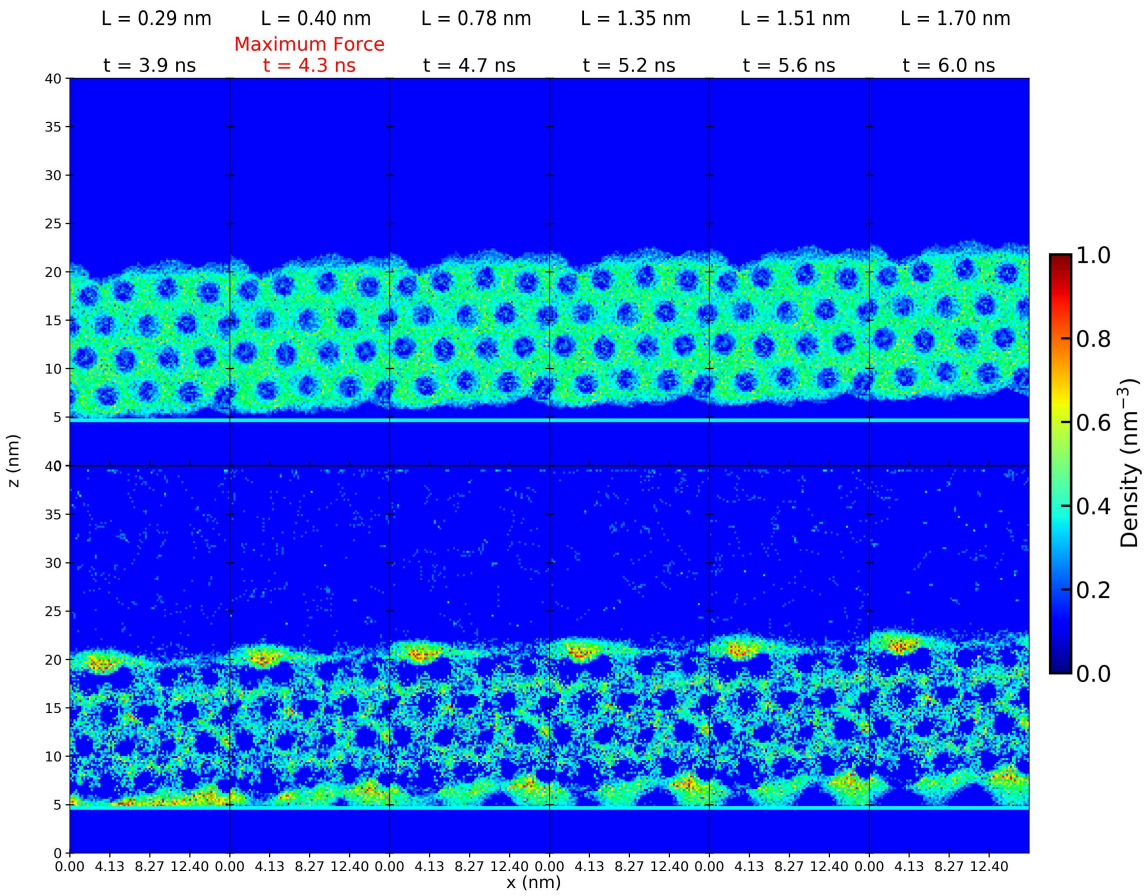

Figure S4: Density profiles of the weakly hydrophilic gecko keratin on the wet surface during pull-off. The 2D density profile of the keratin is shown on the top and the water density profile is shown at the bottom. Going from left to right density plots were calculated at different times during the pull-off. The unbinding event, the moment of maximum pull-off force, is marked in red on the top at a displacement of $L = z_{\mathrm{COM}}(t) - z_{\mathrm{COM,EQ}} = 0.4$ nm, with z_{COM} the position of the center of mass of the top layer nanofibrils. The Gibbs dividing surface of the alkane tails is shown as a horizontal cyan line. Convex capillary bridges can be seen in the bottom density profile of water, between the Gibbs dividing surface of the alkanes and the keratin.

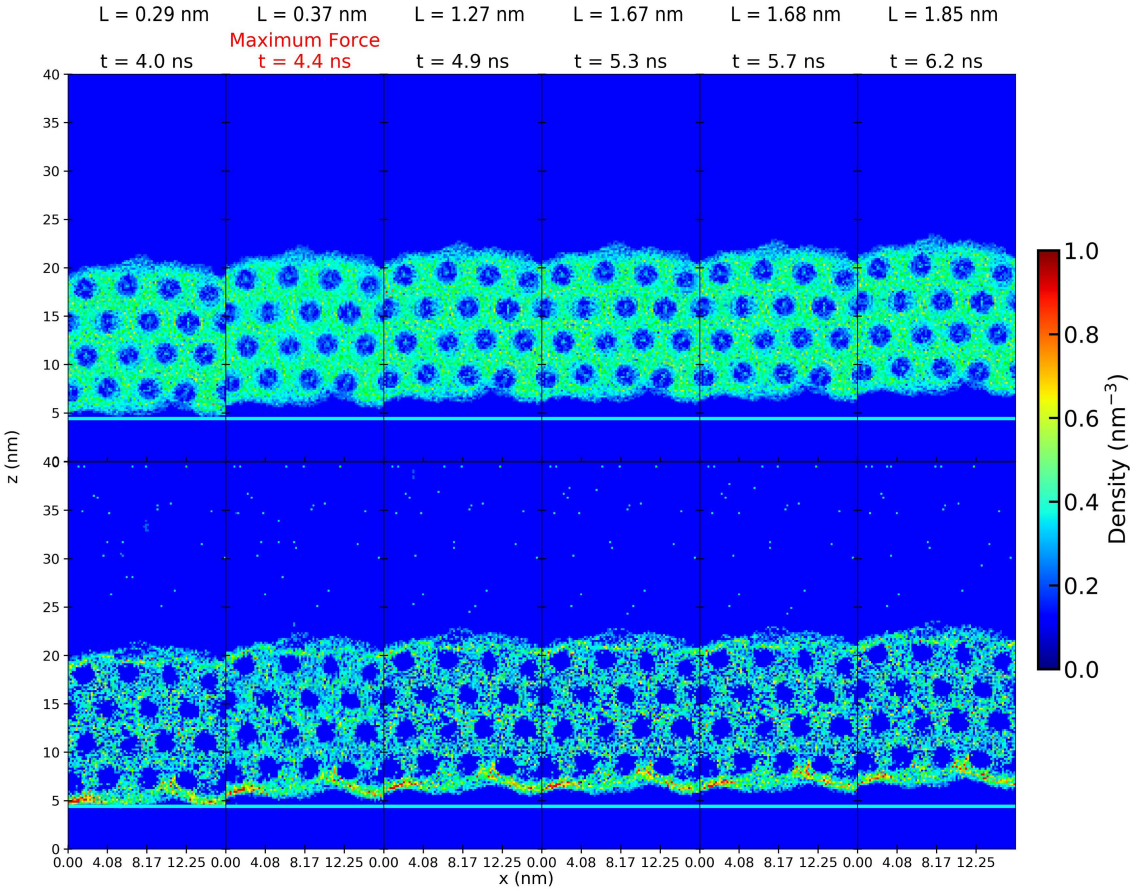

Figure S5: Density profiles of the strongly hydrophilic gecko keratin on the wet surface during pull-off. The 2D density profile of the keratin is shown on the top and the water density profile is shown at the bottom. Going from left to right density plots were calculated at different times during the pull-off. The unbinding event, the moment of maximum pull-off force, is marked in red on the top at a displacement of $L = z_{\mathrm{COM}}(t) - z_{\mathrm{COM,EQ}} = 0.37$ nm, with z_{COM} the position of the center of mass of the top layer nanofibrils. The Gibbs dividing surface of the alkane tails is shown as a horizontal cyan line. The keratin is pulled straight of the surface, without the formation of capillary bridges.

References

(1) Endoh, K. S.; Kawakatsu, T.; Müller-Plathe, F. Coarse-Grained Molecular Simulation Model for Gecko Feet Keratin. *J. Phys. Chem. B* **2018**, *122*, 2203–2212, DOI: 10.1021/acs.jpcb.7b10481.

(2) Berendsen, H. J. C.; Postma, J. P. M.; van Gunsteren, W. F.; DiNola, A.; Haak, J. R. Molecular dynamics with coupling to an external bath. *J. Chem. Phys.* **1984**, *81*, 3684–3690, DOI: 10.1063/1.448118.